

ORIGINAL

Open Access

# Decoration of multi-walled carbon nanotubes (MWCNTs) with different ferrite nanoparticles and its use as an adsorbent

Ahmed A Farghali<sup>1</sup>, Mohamed Bahgat<sup>2</sup>, Waleed M A ElRouby<sup>1\*</sup> and Mohamed H Khedr<sup>1</sup>

## Abstract

A simple and inexpensive synthesis route to produce multi-walled carbon nanotubes (MWCNTs) decorated with  $\text{CoFe}_2\text{O}_4$  and  $\text{Co}_{0.5}\text{Ni}_{0.5}\text{Fe}_2\text{O}_4$  nanoparticles using a simplified hydrothermal precipitation is reported. Transmission electron microscopy and X-ray diffraction confirm the formation of 14.9 nm  $\text{CoFe}_2\text{O}_4$  and 26 nm  $\text{Co}_{0.5}\text{Ni}_{0.5}\text{Fe}_2\text{O}_4$  nanoparticles on MWCNTs surface. The prepared composite was used for methyl green adsorption. The effects of various parameters, such as temperature, initial dye concentration, and composite dosage, were investigated. Experimental results have shown that the amount of adsorbed dye increased with increasing initial dye concentration, composite dosage, and temperature. The adsorption kinetic data were analyzed using pseudo-first-order, pseudo-second-order, and intraparticle diffusion models. It was found that the pseudo-second-order kinetic model was the most appropriate model in describing the adsorption kinetics. The adsorption isotherms of methyl green onto MWCNTs decorated with  $\text{CoFe}_2\text{O}_4$  and  $\text{Co}_{0.5}\text{Ni}_{0.5}\text{Fe}_2\text{O}_4$  nanoparticles were determined at 298, 313, and 323 K. Equilibrium data were fitted to the Langmuir and the Freundlich isotherm models, then the isotherm constants were determined. The equilibrium data were best represented by the Langmuir isotherm model. Thermodynamic parameters such as changes in the free energy of adsorption, enthalpy, entropy, and activation energy were calculated.

**Keywords:** MWCNTs; Decoration;  $\text{CoFe}_2\text{O}_4$ ;  $\text{Co}_{0.5}\text{Ni}_{0.5}\text{Fe}_2\text{O}_4$ ; Methyl green; Adsorption

## Background

Many industries, such as textile, paper, plastic, and dyestuffs, consume substantial amount of water and also use chemicals and dyes to color their products during the manufacturing process [1,2]. Color is the first contaminant recognized in wastewater, and the presence of very small amounts of dyes in water is highly visible and undesirable [3]. Most of these dyes contain aromatic rings, which make them carcinogenic and mutagenic [4,5]. Therefore, the removal of dyes is currently of high importance for environmental remediation. Adsorption technology is one of the most effective methods for dye and toxic removal due to its low cost, high efficiency, simplicity, and insensitivity to toxic substances [6,7].

Due to their large specific surface area and small, hollow, and layered structures, nanomaterials have recently drawn much attention for dye removal applications. For instance, carbon nanotubes (CNTs) are attracting increasing research interest as promising adsorbents for harmful cations, anions, and other organic and inorganic impurities present in natural sources of water [8-10]. However, it is difficult to separate CNTs from aqueous solutions because of their small size. There are serious concerns over the health and environmental risks of CNTs once they have been released into the environment [11]. It should be noted that CNTs can enter cells, causing damage to plants, animals, and human beings [12]. Thus, there is potential for CNTs to become another source of environmental contaminant if the use of CNTs is not responsibly managed. Compared with traditional centrifugation and filtration methods, the magnetic separation method is considered as a rapid and

\* Correspondence: waleedmohamedali@yahoo.com

<sup>1</sup>Nanotechnology Department, Faculty of Postgraduate Studies for Advanced Sciences, Beni-Suef University, Beni-Suef 62111, Egypt

Full list of author information is available at the end of the article

effective technique for separating adsorbents from environmental applications [13].

Magnetic separation technology is a fast and easy method for separating magnetic adsorbents from an aqueous solution. In recent years, magnetic separation technology, combined with the adsorption process, has been widely used for dye removal from wastewaters [14-16]. To date, only a few studies have been conducted on the adsorption of dyes by magnetic CNTs. Qu et al. have prepared multi-walled carbon nanotubes (MWCNTs) filled with  $\text{Fe}_2\text{O}_3$  for removal of methylene blue and neutral red from aqueous solution [17]. Gong et al. have synthesized magnetic MWCNT nanocomposites as adsorbent for the removal of cationic dyes: methylene blue, neutral red, and brilliant cresyl from aqueous solution [18]. Madrakian et al. used magnetic-modified MWCNTs for the removal of cationic dye crystal violet, thionine, janus green B, and methylene blue from water samples [19].

In the present work, the main purpose is to demonstrate a simple and general procedure for the decoration of MWCNTs with magnetic ferrite ( $\text{CoFe}_2\text{O}_4$  or  $\text{Co}_{0.5}\text{Ni}_{0.5}\text{Fe}_2\text{O}_4$ ). The decorated MWCNTs were used and evaluated as possible sorbents for the removal of methyl green from aqueous solution. The effect of methyl green concentration, temperature, and contact time on the adsorption process was investigated. Kinetics and thermodynamics studies have been performed, and the results have been analyzed. Thermodynamic parameters, such as  $\Delta G^0$ ,  $\Delta H^0$ , and  $\Delta S^0$ , were calculated.

## Results and discussion

### Characterizations of synthesized materials

Figure 1 shows TEM images of the pure and decorated MWCNTs. Figure 1a shows the morphological structure of MWCNTs where the crystalline tubular structure of nanotubes are observed. It is observed that the nanotubes have clear inner channels with lengths of some microns. Figure 1b displays typical TEM images of MWCNTs decorated with  $\text{CoFe}_2\text{O}_4$  nanoparticles. It shows the morphology and the size distribution of  $\text{CoFe}_2\text{O}_4$  nanoparticles. It can be seen that the size of nanoparticles is distributed from 8.3 to 18.9 nm, and the mean particle size is about 14.9 nm.  $\text{CoFe}_2\text{O}_4$  nanoparticles are seen as dense aggregates. The well-distributed nanoparticles deposited onto the carbon nanotubes demonstrate that the MWCNTs pretreatment processing was effective, which resulted in many active sites on the carbon nanotubes. Figure 1c shows the typical TEM image of MWCNTs decorated with  $\text{Co}_{0.5}\text{Ni}_{0.5}\text{Fe}_2\text{O}_4$  nanoparticles.  $\text{Co}_{0.5}\text{Ni}_{0.5}\text{Fe}_2\text{O}_4$  nanoparticles dispersed on the sidewalls of the carbon nanotubes and the inner cavity of the tube still clear.

In X-ray diffraction (XRD) patterns of  $\text{CoFe}_2\text{O}_4$  and  $\text{CoFe}_2\text{O}_4/\text{MWCNTs}$  the diffraction peak at  $18.4^\circ$ ,

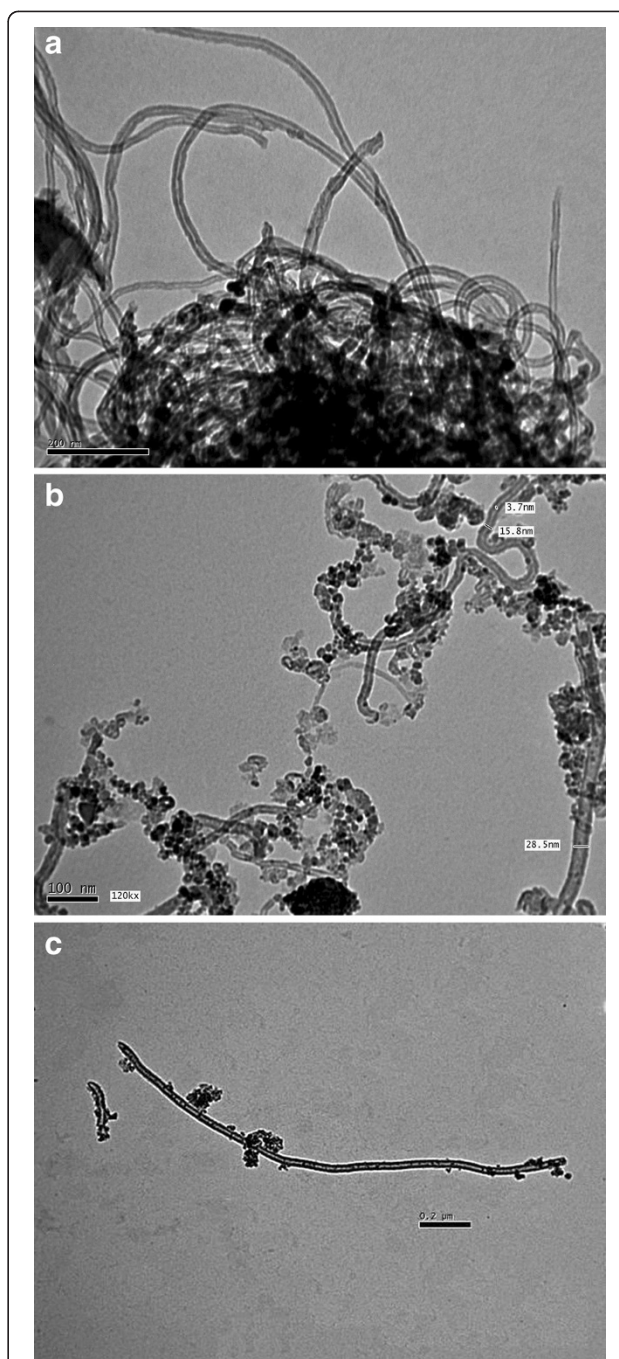


**Figure 1** TEM images of pure MWCNT and MWCNT decorated with  $\text{CoFe}_2\text{O}_4$  nanoparticles and with  $\text{Co}_{0.5}\text{Ni}_{0.5}\text{Fe}_2\text{O}_4$  nanoparticles. Pure MWCNT (a), MWCNTs decorated with  $\text{CoFe}_2\text{O}_4$  nanoparticles (b), and MWCNTs decorated with  $\text{Co}_{0.5}\text{Ni}_{0.5}\text{Fe}_2\text{O}_4$  nanoparticles (c).

$30.09^\circ$ ,  $35.55^\circ$ ,  $43.018^\circ$ ,  $57.08^\circ$ , and  $62.66^\circ$  are reflections of  $\text{CoFe}_2\text{O}_4$ . Nevertheless, in XRD patterns of  $\text{CoFe}_2\text{O}_4/\text{MWCNTs}$ , the additional peaks could be well seen at  $26.066^\circ$  which is corresponding to graphite (Figure 2).

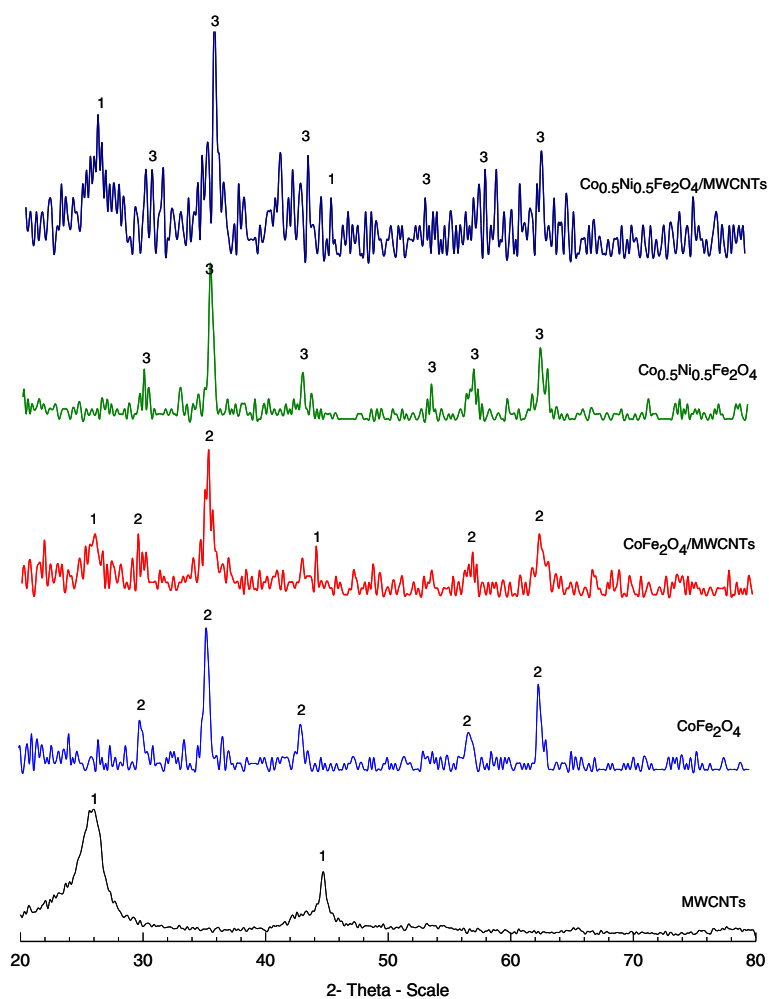


**Figure 2** XRD diffraction patterns of MWCNTs,  $\text{CoFe}_2\text{O}_4$ ,  $\text{CoFe}_2\text{O}_4/\text{MWCNTs}$ ,  $\text{Co}_{0.5}\text{Ni}_{0.5}\text{Fe}_2\text{O}_4$  and  $\text{Co}_{0.5}\text{Ni}_{0.5}\text{Fe}_2\text{O}_4/\text{MWCNTs}$ . 1. Graphite, 2.  $\text{CoFe}_2\text{O}_4$ , 3.  $\text{Co}_{0.5}\text{Ni}_{0.5}\text{Fe}_2\text{O}_4$ .

The crystallite size of  $\text{CoFe}_2\text{O}_4$  on MWCNTs surface was calculated using the Scherer equation (Equation 1) [20].

$$D = 0.89\lambda / B \cos\theta, \quad (1)$$

where  $\lambda = 0.154056$  nm, B is the full peak width at half maximum value, and  $\theta$  is the diffraction angle.

It was found that the average crystallite size is about 14.9 nm. XRD patterns of  $\text{Co}_{0.5}\text{Ni}_{0.5}\text{Fe}_2\text{O}_4$  and  $\text{Co}_{0.5}\text{Ni}_{0.5}\text{Fe}_2\text{O}_4/\text{MWCNTs}$  were also shown in Figure 2. The sample exhibits characteristic diffraction peaks of  $\text{Co}_{0.5}\text{Ni}_{0.5}\text{Fe}_2\text{O}_4$  at  $2\theta$  of  $30.22^\circ$ ,  $35.6^\circ$ ,  $43.18^\circ$ ,  $57.28^\circ$ , and  $62.84^\circ$ , but in XRD of  $\text{Co}_{0.5}\text{Ni}_{0.5}\text{Fe}_2\text{O}_4/\text{MWCNTs}$ , there is an additional peak at  $26.066^\circ$  which is corresponding to graphite. The average crystallite size of the  $\text{Co}_{0.5}\text{Ni}_{0.5}\text{Fe}_2\text{O}_4$  particles is determined using the Scherer equation and found it to be about 26.2 nm.

Fourier transform infrared spectroscopic analysis of oxidized MWCNTs has been shown in Figure 3. The Fourier transform infrared spectroscopy (FTIR) study of

oxidized MWCNTs confirms the defective sites at the surface of MWCNTs, and the presence of function groups  $>C=C$  ( $1,642/\text{cm}$ ),  $>C=O$  ( $1,025/\text{cm}$ ),  $=\text{CH}_2$  ( $2,857/\text{cm}$ ,  $2,925/\text{cm}$ ), and  $-\text{OH}$  ( $3,439/\text{cm}$ ). This leads to the hydrophilic nature of MWCNTs. These functional

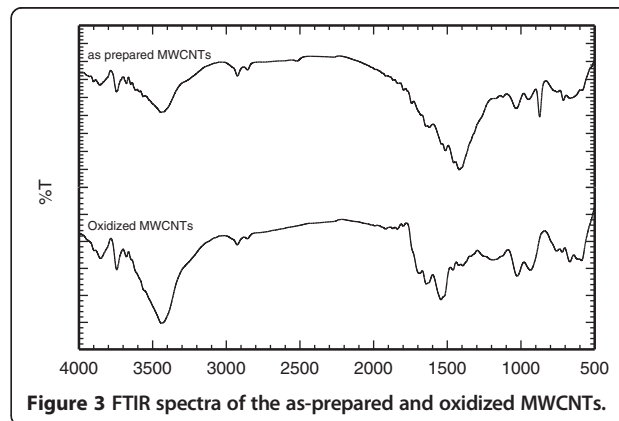


**Figure 3** FTIR spectra of the as-prepared and oxidized MWCNTs.

groups may also act as anchoring sites for ferrite particles in the decoration process and also in the adsorption of dye molecules.

N<sub>2</sub> adsorption-desorption isotherm of MWCNTs decorated with CoFe<sub>2</sub>O<sub>4</sub> and MWCNTs decorated with Co<sub>0.5</sub>Ni<sub>0.5</sub>Fe<sub>2</sub>O<sub>4</sub> nanoparticles are shown in Figure 4. There are hysteresis loops clearly visible in the isotherm, which is associated with capillary condensation in mesopores. These mesopores include mesopore-sized inner cavities and aggregated pores resulted from aggregation of decorated MWCNTs. Surface area by the Brunauer-Emmett-Teller (BET) method, micropore volume by the t-plot method, and pore size distributions by the BJH equation are obtained for MWCNTs decorated with CoFe<sub>2</sub>O<sub>4</sub> and Co<sub>0.5</sub>Ni<sub>0.5</sub>Fe<sub>2</sub>O<sub>4</sub> as listed in Table 1. This adsorption isotherm exhibited a type-II shape. It was observed that there was a small closed adsorption-desorption hysteresis loop with a relative pressure above 0.4, which is suggested to be due to the mesopores with a capillary condensation [21].

#### Adsorption of methyl green dye

##### *Effect of adsorbent dosage on adsorption capacity of methyl green*

The mechanism of MWCNT adsorption for methyl green dyes may be derived from two reasons: the first reason might be based on the van der Waals interactions occurring between the hexagonally arrayed carbon atoms in the graphite sheet of MWCNTs and the aromatic backbones of the dyes [22]; the second reason might be due to the electrostatic attraction between the

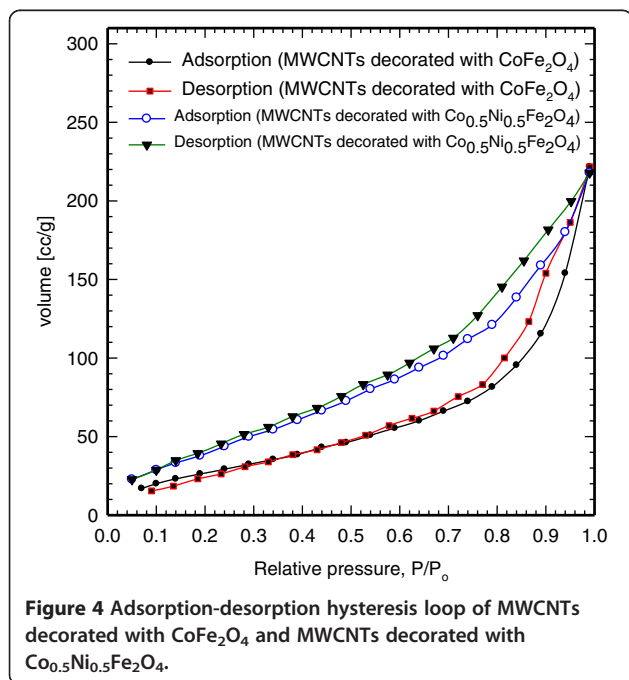


**Figure 4** Adsorption-desorption hysteresis loop of MWCNTs decorated with CoFe<sub>2</sub>O<sub>4</sub> and MWCNTs decorated with Co<sub>0.5</sub>Ni<sub>0.5</sub>Fe<sub>2</sub>O<sub>4</sub>.

**Table 1** Surface area measurements for MWCNTs decorated with CoFe<sub>2</sub>O<sub>4</sub> and MWCNTs decorated with Co<sub>0.5</sub>Ni<sub>0.5</sub>Fe<sub>2</sub>O<sub>4</sub> nanoparticles

Measurement	MWCNT decorated with CoFe <sub>2</sub> O <sub>4</sub>	MWCNT decorated with Co <sub>0.5</sub> Ni <sub>0.5</sub> Fe <sub>2</sub> O <sub>4</sub>
Surface area (m <sup>2</sup> /g)	109.54	176
Total pore volume (cm <sup>3</sup> /g)	0.0505	0.076
Average pore diameter (nm)	18.96	17.33
Micro pore volume (cm <sup>3</sup> /g)	0.109	0.16

positive cationic dyes and the negative charged MWCNTs adsorbent surface.

It was observed that the percentages of adsorbed dye increased as the decorated MWCNT dosages were increased over the range 0.6 to 1.4 g/L as shown in Figure 5. The increase in the percentage of the removed dye with an adsorbent dosage can be attributed to an increase in the adsorbent surface, which increased the availability of the adsorption sites.

##### *Effects of dye concentration*

The amount of adsorbed dye per unit of decorated MWCNT mass increased as initial dye concentration increased due to the increase in the driving force of the concentration gradient as shown in Figure 6. The adsorption process at different concentrations was rapid in the initial 30 min then gradually decreased as adsorption proceeded until equilibrium was reached. This progression is expected to be based on the large number of vacant surface sites available for adsorption during the initial stage. After a certain time, the remaining vacant surface sites are difficult to be occupied due to the repulsive forces between dye molecules on the decorated MWCNTs and bulk phases [23].

##### *Effect of temperature*

To study the effect of temperature on the adsorption of methyl green dye onto MWCNTs decorated with CoFe<sub>2</sub>O<sub>4</sub> or Co<sub>0.5</sub>Ni<sub>0.5</sub>Fe<sub>2</sub>O<sub>4</sub> nanoparticles, the experiments were performed at temperatures of 298, 313, and 323 K as shown in Figure 7. It was observed that the equilibrium adsorption capacity of methyl green onto both decorated MWCNTs increased with increasing the temperature due to increasing the mobility of dye molecules.

Equilibrium uptake increased with the increasing of methylene blue concentrations at the present experimental range. This is a result of the increase in the driving force from the concentration gradient. In the same conditions, if the concentration of methyl green in the

**Table 2 Isotherm parameters for removal of methyl green by the decorated MWCNTs at different temperatures**

Isotherms	Parameters	Temperatures (K)					
		MWCNT decorated with $\text{CoFe}_2\text{O}_4$			MWCNT decorated with $\text{Co}_{0.5}\text{Ni}_{0.5}\text{Fe}_2\text{O}_4$		
		298 K	313 K	323 K	298 K	313 K	323 K
Langmuir	$q_0$ (mg/g)	91.74	96.16	103.3	172.98	244.25	257.7
	$K_L$ (L/mg)	0.0556	0.0698	0.0822	0.072	0.088	0.102
	$R_L$	0.043	0.0345	0.095	0.0335	0.0276	0.024
	$R^2$	0.997	0.997	0.995	0.992	0.991	0.992
Freundlich	$K_F$ (mg/g (L/mg) <sup>1/n</sup> )	19.98	22.264	22.624	42.52	51.94	65.75
	$n$	3.57	3.62	3.67	3.89	3.3	3.79
	$R^2$	0.926	0.902	0.900	0.98	0.95	0.96

solution was bigger, the active sites of MWCNTs decorated with  $\text{CoFe}_2\text{O}_4$  or  $\text{Co}_{0.5}\text{Ni}_{0.5}\text{Fe}_2\text{O}_4$  nanoparticles were surrounded by much more methyl green ions, and the process of adsorption would be carried out sufficiently. Therefore, the amount absorbed at equilibrium ( $q_e$ ) increased with the increase in equilibrium methyl green concentrations. From Figure 7, the adsorption capacity of methyl green onto MWCNTs decorated with  $\text{CoFe}_2\text{O}_4$  are 85.07, 89.41, and 96.24 mg/g at 298, 313, and 323 K, respectively, while the adsorption capacity for MWCNTs decorated with  $\text{Co}_{0.5}\text{Ni}_{0.5}\text{Fe}_2\text{O}_4$  are 167.95, 288.40, and 243.89 mg/g at 298, 313, and 323 K, respectively. The increase of the equilibrium adsorption with the increase in temperature indicated that the adsorption of methyl green ions onto  $\text{CoFe}_2\text{O}_4/\text{MWCNT}$  composite was endothermic in nature. The higher adsorption capacity of

MWCNTs decorated with  $\text{Co}_{0.5}\text{Ni}_{0.5}\text{Fe}_2\text{O}_4$  than MWCNTs decorated with  $\text{CoFe}_2\text{O}_4$  may be attributed to the high surface area of MWCNTs decorated with  $\text{Co}_{0.5}\text{Ni}_{0.5}\text{Fe}_2\text{O}_4$  or may be due to the small crystallite size of  $\text{CoFe}_2\text{O}_4$  nanoparticles on the MWCNTs surface which can act as a blocker for the active sites on the tube surfaces (Figure 1).

**Adsorption isotherms**

The quantity of the dye that could be adsorbed over MWCNTs decorated with  $\text{CoFe}_2\text{O}_4$  or  $\text{Co}_{0.5}\text{Ni}_{0.5}\text{Fe}_2\text{O}_4$  nanoparticles surface is a function of concentration, which could be explained by the adsorption isotherms. In the present study, the Langmuir [24] and Freundlich [25] isotherms are tested for methyl green dye adsorption.

The Langmuir adsorption isotherm assumes that adsorption takes place at specific homogeneous sites

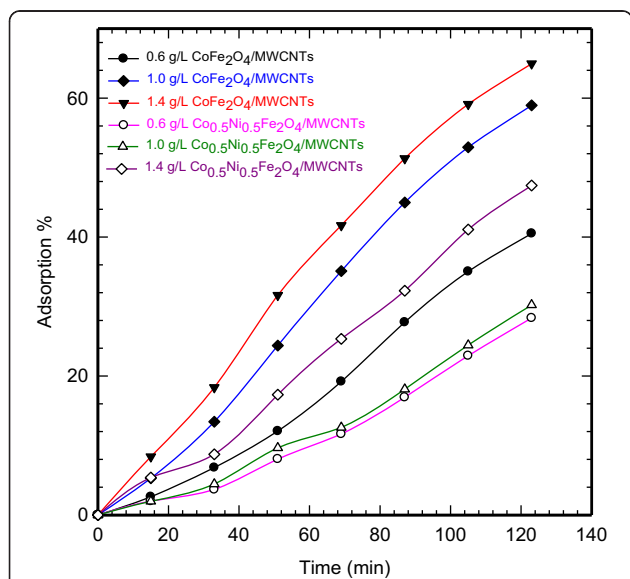


**Figure 5 Effects of decorated MWCNT dosages on the adsorption of methyl green dye.** Dye concentration = 100 mg/L and  $T = 298$  K.

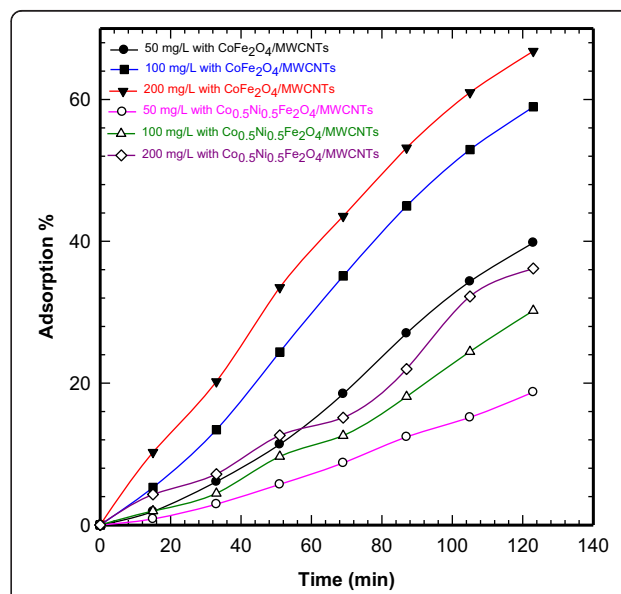
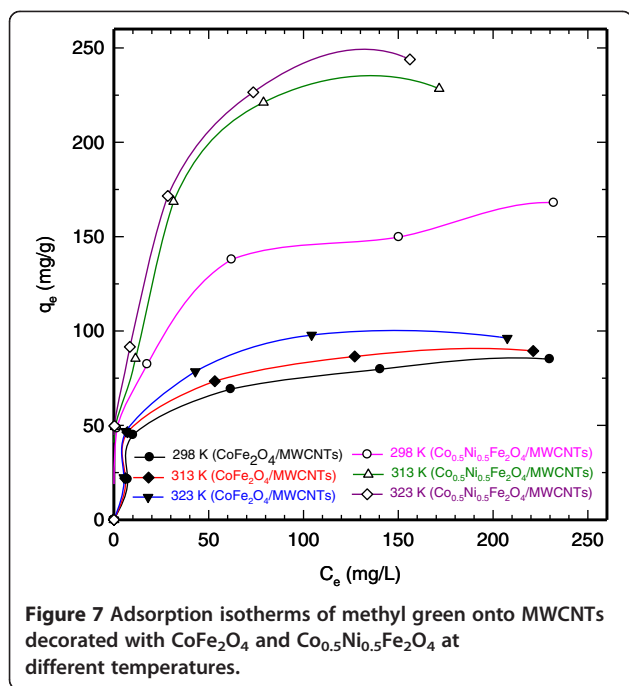


**Figure 6 Effects of dye concentration on the adsorption of methyl green dye.**  $\text{CoFe}_2\text{O}_4/\text{MWCNTs}$  and  $\text{Co}_{0.5}\text{Ni}_{0.5}\text{Fe}_2\text{O}_4/\text{MWCNTs} = 1$  g/L and  $T = 298$  K.



within the adsorbent. The Langmuir isotherm can be written in this form:

$$C_e/q_e = 1/(q_0K_L) + (1/q_0)C_e, \quad (2)$$

where  $C_e$  (mg/L) is the equilibrium concentration,  $q_e$  (mg/g) is the amount of adsorbate adsorbed per unit mass of adsorbate, and  $q_0$  and  $K_L$  are the Langmuir constants related to the adsorption capacity and the rate of adsorption, respectively. When  $C_e/q_e$  was plotted against  $C_e$ , a straight line with slope  $1/q_0$  was obtained (Figure 8a,c), indicating that the adsorption of methyl green onto MWCNTs decorated with  $\text{CoFe}_2\text{O}_4$  or  $\text{Co}_{0.5}\text{Ni}_{0.5}\text{Fe}_2\text{O}_4$  nanoparticles follows the Langmuir isotherm. The Langmuir constants  $K_L$  and  $q_0$  were calculated from this isotherm, and their values are listed in Table 2. Another important parameter,  $R_L$ , is called the separation factor or the equilibrium parameter which is determined from the relation [26]:

$$R_L = 1/ [1 + K_L C_o] \quad (3)$$

where  $K_L$  is the Langmuir constant (l/mg) and  $C_o$  (mg/L) is the highest dye concentration. The value of  $R_L$  indicates the type of the isotherm to be either unfavorable ( $R_L > 1$ ), linear ( $R_L = 1$ ), favorable ( $0 < R_L < 1$ ), or irreversible ( $R_L = 0$ ).  $R_L$  values for methyl green adsorption onto MWCNTs decorated with  $\text{CoFe}_2\text{O}_4$  or  $\text{Co}_{0.5}\text{Ni}_{0.5}\text{Fe}_2\text{O}_4$  nanoparticles were calculated and found to be less than 1 and greater than zero indicating the favorable adsorption (Table 2).

The Freundlich isotherm is an empirical equation employed to describe the heterogeneous systems [27]. The Freundlich equation is as follows:

$$\ln q_e = \ln K_F + (1/n)\ln C_e, \quad (4)$$

where  $q_e$  is the amount adsorbed at equilibrium (mg/g) and  $C_e$  is the equilibrium concentration of methyl green.  $n$  and  $K_F$  are Freundlich constants,  $n$  giving an indication of how favorable the adsorption process and  $K_F$  (mg/g (L/mg) $^{1/n}$ ) is the adsorption capacity of the adsorbent. The slope  $1/n$  ranging between 0 and 1 is a measure of the adsorption intensity or the surface heterogeneity, becoming more heterogeneous as its value gets closer to 0 [28]. The plot of  $\ln q_e$  versus  $\ln C_e$  (Figure 8b,c) gives straight lines with slope  $1/n$  reflecting that the adsorption of methyl green also follows the Freundlich isotherm. Accordingly, Freundlich constants ( $K_F$  and  $n$ ) were calculated and listed in Table 2.

#### Kinetics analyses

The kinetic analysis of temperature effect was evaluated. The adsorption capacity increased with the temperature, indicating that the mobility of dye molecules increased with temperature, and the adsorption was endothermic. Additionally, increasing the temperature reduces the viscosity of the solution and increases the diffusion rate of dye molecules.

The pseudo-first-order, pseudo-second-order, and intraparticle diffusion models were adopted to test the experimental data and thereby elucidated the kinetic adsorption process. The pseudo first-order model can be expressed as follows:

$$\ln(q_e - q) = \ln(q_e) - k_1 t, \quad (5)$$

where  $q_e$  and  $q$  are the amounts of methyl green adsorbed on MWCNTs decorated with  $\text{CoFe}_2\text{O}_4$  or  $\text{Co}_{0.5}\text{Ni}_{0.5}\text{Fe}_2\text{O}_4$  nanoparticles at equilibrium and at various times  $t$  (mg/g) and  $k_1$  is the rate constant of the pseudo-first-order model for the adsorption (per minute) [29]. The values of  $q_e$  and  $k_1$  can be determined from the intercept and the slope of the linear plot of  $\ln(q_e - q)$  versus  $t$  (Figure 9a,b).

The pseudo-second-order model is as follows:

$$t/q = 1/k_2 q_e^2 + t/q_e, \quad (6)$$

where  $q_e$  and  $q$  are the amounts of dye adsorbed onto MWCNTs decorated with  $\text{CoFe}_2\text{O}_4$  or  $\text{Co}_{0.5}\text{Ni}_{0.5}\text{Fe}_2\text{O}_4$  nanoparticles at equilibrium and at various times  $t$  (mg/g), and  $k_2$  is the rate constant of the pseudo-second-order model for adsorption (g/mg/min) [29]. The slope and intercept of the linear plot of  $t/q$  as a function of  $t$  (Figure 9c,d) yielded the values of  $q_e$  and  $k_2$ . Additionally,

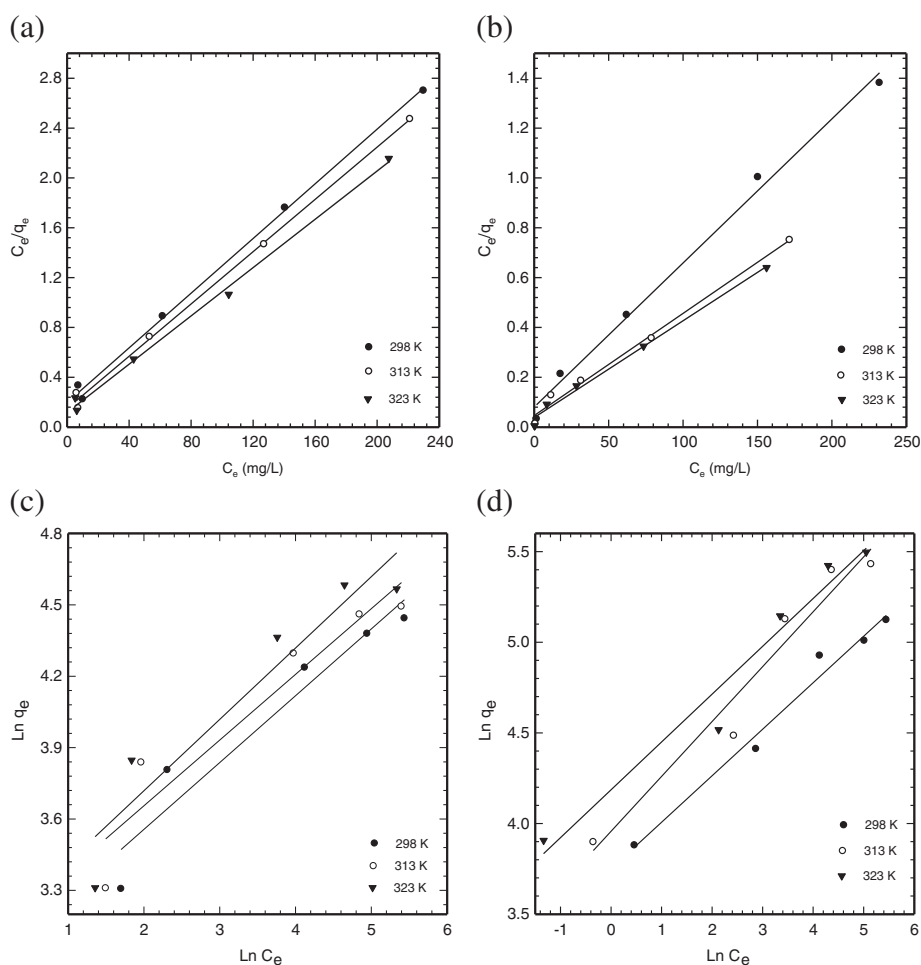


**Figure 8** Langmuir isotherms and Freundlich isotherms. Langmuir isotherms (a,c) for MWCNTs decorated with  $\text{CoFe}_2\text{O}_4$  and  $\text{Co}_{0.5}\text{Ni}_{0.5}\text{Fe}_2\text{O}_4$  nanoparticles, respectively, and Freundlich isotherms (b,d) for MWCNTs decorated with  $\text{CoFe}_2\text{O}_4$  and  $\text{Co}_{0.5}\text{Ni}_{0.5}\text{Fe}_2\text{O}_4$  nanoparticles, respectively, for methyl green dye adsorption at different temperatures.

**Table 3** Coefficients of pseudo-first and second-order adsorption kinetic models and intraparticle diffusion model (methyl green = 100 mg/L, MWCNTs decorated with  $\text{CoFe}_2\text{O}_4$  or  $\text{Co}_{0.5}\text{Ni}_{0.5}\text{Fe}_2\text{O}_4 = 1 \text{ g/L}$ )

Orders model	Parameters	Temperatures (K)					
		MWCNT decorated with $\text{Co}_{0.5}\text{Ni}_{0.5}\text{Fe}_2\text{O}_4$			MWCNT decorated with $\text{CoFe}_2\text{O}_4$		
		298 K	323 K	313 K	298 K	323 K	313 K
Pseudo-first-order model	$q_e \text{ Cal. (mg/g)}$	51.92	87.452	83.12	80.125	19.22	30.96
	$q_e \text{ Exp. (mg/g)}$	44.96	91.59	85.40	82.39	47.58	46.43
	$K_1 \text{ (min}^{-1}\text{)}$	9.747	$5.29 \times 10^{-3}$	$4.26 \times 10^{-3}$	$3.28 \times 10^{-3}$	0.013	0.014
	$R^2$	0.99	0.977	0.99	0.985	0.90	0.977
Pseudo-second-order model	$q_e \text{ Cal. (mg/g)}$	45.15	87.452	83.12	80.125	74.6	46.55
	$q_e \text{ Exp. (mg/g)}$	44.96	91.59	85.40	82.39	47.58	46.43
	$K_2 \text{ (g/mg min)}$	0.00046	$1.08 \times 10^{-4}$	$7.66 \times 10^{-5}$	$6.15 \times 10^{-5}$	0.0012	0.00092
	$R^2$	0.995	0.992	0.998	0.991	0.998	0.998
Intraparticle diffusion model	$k_i \text{ (mg/g min}^{0.5}\text{)}$	3.214	4.98	4.061	3.4	2.05	2.958
	$C \text{ (mg/g)}$	0.591	-7.685	-8.66	-12.056	22.44	9.22
	$R^2$	0.981	0.991	0.999	0.997	0.90	0.958

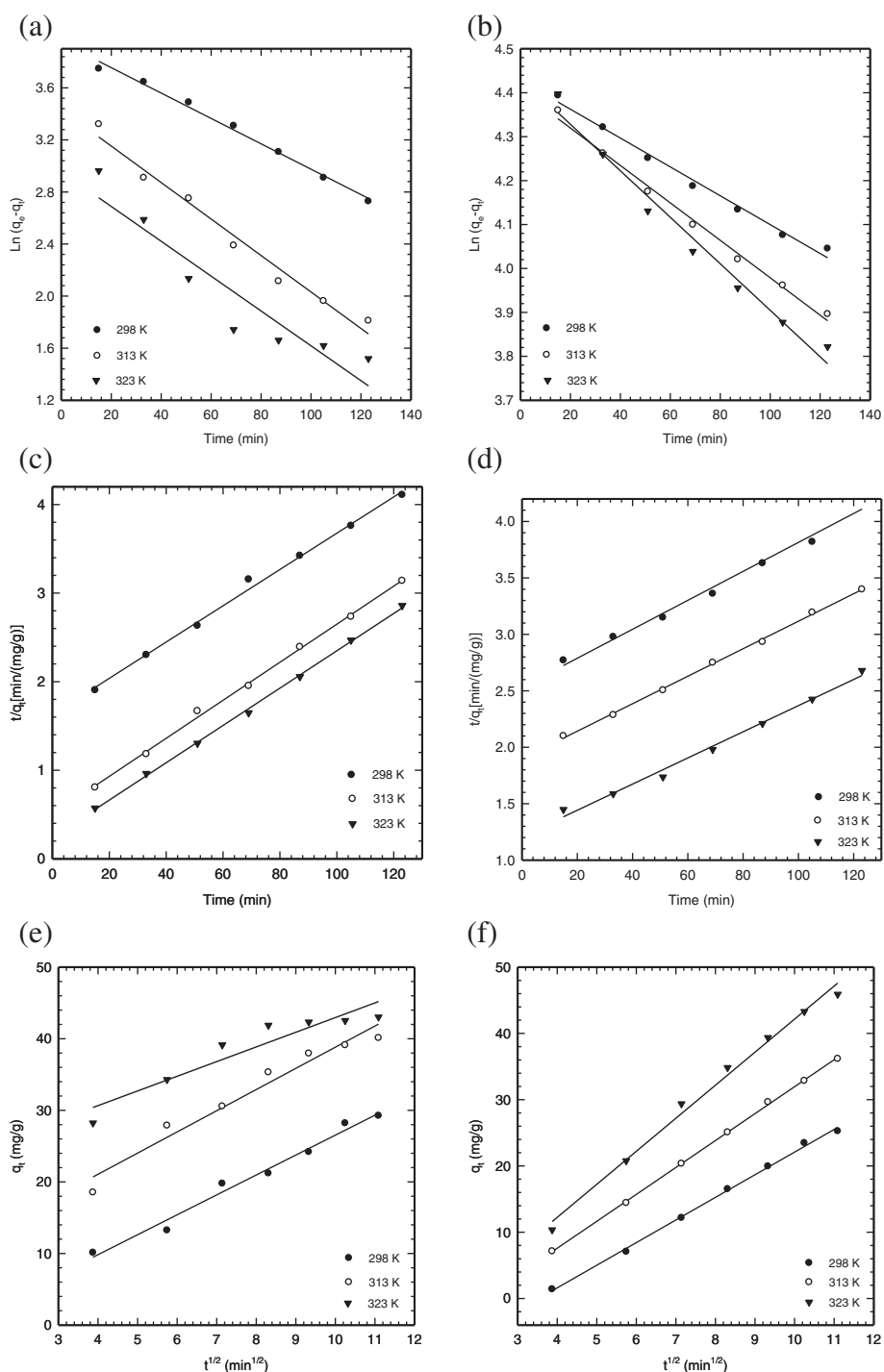


**Figure 9** Regressions of kinetic plots at different temperatures. Pseudo-first-order model **(a)**  $\text{CoFe}_2\text{O}_4/\text{MWCNTs}$ , **(b)**  $\text{Co}_{0.5}\text{Ni}_{0.5}\text{Fe}_2\text{O}_4/\text{MWCNTs}$ ; pseudo-second-order model **(c)**  $\text{CoFe}_2\text{O}_4/\text{MWCNTs}$ , **(d)**  $\text{Co}_{0.5}\text{Ni}_{0.5}\text{Fe}_2\text{O}_4/\text{MWCNTs}$ ; intraparticle diffusion model **(e)**  $\text{CoFe}_2\text{O}_4/\text{MWCNTs}$ , **(f)**  $\text{Co}_{0.5}\text{Ni}_{0.5}\text{Fe}_2\text{O}_4/\text{MWCNTs}$ .

the initial adsorption rate  $h$  (mg/g/min) can be determined using the equation  $h = k_2 q_e^2$ . The adsorption process on porous adsorbents generally has a four-stage bulk diffusion, film diffusion, intraparticle

diffusion, and finally, adsorption of the solute onto the surface. Typically, bulk diffusion and adsorption are assumed to be rapid and therefore not rate determining. Since the pseudo-second-order model cannot



identify the diffusion mechanism, kinetic results were analyzed using the intraparticle diffusion model to elucidate the diffusion mechanism. Film diffusion was negligible, and intraparticle diffusion was the only rate-controlling step. The intraparticle diffusion model is expressed as follows:

$$q = k_i t^{1/2} + C, \quad (7)$$

where  $C$  is the intercept and  $k_i$  is the intraparticle diffusion rate constant ( $\text{mg/g/min}^{0.5}$ ), which can be determined from the slope of the linear plot of  $q$  versus  $t^{1/2}$  [30] (Figure 9e,f). Table 3 presents the kinetic parameters for the removal of methyl green by MWCNTs decorated with  $\text{CoFe}_2\text{O}_4$  or  $\text{Co}_{0.5}\text{Ni}_{0.5}\text{Fe}_2\text{O}_4$  nanoparticles. The  $R^2$  value of the pseudo-second-order model exceeded 0.99; moreover, the  $q$  value ( $q_{\text{ecal}}$ ) derived from the pseudo-second-order model was consistent with the experimental  $q$  values ( $q_{\text{enexp}}$ ). Hence, this study showed that the pseudo-second-order model best represents adsorption kinetics. A similar phenomenon has been observed in the adsorption of Acid Blue 93 by natural sepiolite [31], and Acid Red 57 by surfactant-modified sepiolite [32]. If the regression of  $q$  versus  $t^{1/2}$  is linear and passes through the origin, intraparticle diffusion is then the sole rate-limiting step [32]. Although the regression was linear, the plot did not pass through the origin (Table 3), indicating that adsorption involved intraparticle diffusion that was not the only rate-controlling step. Other kinetic mechanisms may control the adsorption rate, which is a similar finding to that obtained from other studies of adsorption [31]. The values of  $C$  were helpful in determining the boundary thickness: a larger  $C$  value corresponds to a greater boundary layer diffusion effect [33]. The  $C$  values increased with the temperature (298 to 323 K), and so, increasing the temperature promoted the boundary-layer diffusion effect.

#### Adsorption thermodynamics

The thermodynamic parameters, namely free energy ( $\Delta G^\circ$ ), enthalpy ( $\Delta H^\circ$ ), and entropy ( $\Delta S^\circ$ ) have an important role to determine spontaneity and heat change for the

adsorption process. Thermodynamic parameters were calculated using the following relations [34]:

$$\Delta G^\circ = -RT \ln(K_L), \quad (8)$$

$$\ln(K_L) = (\Delta S^\circ / R) - (\Delta H^\circ / RT), \quad (9)$$

where  $K_L$  is the Langmuir equilibrium constant (L/mol),  $R$  is the gas constant (8.314 J/mol/K), and  $T$  is the temperature (K).  $\Delta H^\circ$  and  $\Delta S^\circ$  parameters can be calculated from the slope and intercept of the plot  $\ln K_L$  versus  $1/T$ . From Equation 10,  $\Delta G^\circ$  was calculated using  $\ln K_L$  values for different temperatures. Results are summarized in Table 4. It can be seen that  $\Delta G^\circ$  values at temperatures 298, 313, and 323 K are negative. Hence, the adsorption process was a spontaneous process. The decrease in  $\Delta G^\circ$  value with the increase of temperature indicates the efficient adsorption at higher temperature. The positive  $\Delta H^\circ$  value reflected that the adsorption process is endothermic, and there is a strong interaction between MWCNTs decorated with  $\text{CoFe}_2\text{O}_4$  or  $\text{Co}_{0.5}\text{Ni}_{0.5}\text{Fe}_2\text{O}_4$  nanoparticles and methyl green. Since methyl green ions travel through solution and reach the adsorption sites, it is necessary for them to be stripped out (at least partially) of their hydration shell, that requires energy input. Thus, the positive value of  $\Delta H^\circ$  indicates that the adsorption is increasing with temperature. Moreover, the positive value of  $\Delta S^\circ$  indicates that the degrees of freedom increased at the solid-liquid interface during the adsorption of methyl green onto MWCNTs decorated with  $\text{CoFe}_2\text{O}_4$  or  $\text{Co}_{0.5}\text{Ni}_{0.5}\text{Fe}_2\text{O}_4$  nanoparticles and reflected the affinity of the composite toward methyl green ions in aqueous solutions [35].

The pseudo-second-order model was identified as the best kinetic model for the adsorption of methyl green onto MWCNTs decorated with  $\text{CoFe}_2\text{O}_4$  or  $\text{Co}_{0.5}\text{Ni}_{0.5}\text{Fe}_2\text{O}_4$  nanoparticles. Accordingly, the rate constants ( $k_2$ ) of the pseudo-second-order model were adopted to calculate the activation energy of the adsorption process using the Arrhenius equation [36]:

$$\ln(k_2) = \ln(A) - (E_a / RT), \quad (10)$$

where  $k_2$ ,  $A$ ,  $E_a$ ,  $R$ , and  $T$  are the rate constant of the

**Table 4 Thermodynamic parameters of methyl green dye adsorption onto decorated MWCNTs at various temperatures**

Temperature (K)	MWCNT decorated with $\text{CoFe}_2\text{O}_4$				MWCNT decorated with $\text{Co}_{0.5}\text{Ni}_{0.5}\text{Fe}_2\text{O}_4$			
	$\Delta G^\circ$ (kJ/mol)	$\Delta H^\circ$ (kJ/mol)	$\Delta S^\circ$ (J/mol/K)	$E_a$ (kJ/mol)	$\Delta G^\circ$ (kJ/mol)	$\Delta H^\circ$ (kJ/mol)	$\Delta S^\circ$ (J/mol/K)	$E_a$ (kJ/mol)
298	-8.023	31.189	68.64	12.44	-21.7	17.38	35.9	11.075
313	-9.019				-22.27			
323	-9.746				-22.59			

pseudo-second-order model (g/mg/min), the Arrhenius factor, the activation energy (kJ/mol), the gas constant (8.314 J/mol/K), and the temperature (K), respectively. The activation energy could be determined from the slope of the plot of  $\ln(k_2)$  versus  $1/T$  (Table 4). Nollet et al. [37] mentioned that the physisorption process normally had activation energy of 5 to 40 kJ/mol, while chemisorption had higher activation energy (40 to 800 kJ/mol). Therefore,  $\Delta H^\circ$ ,  $\Delta G^\circ$ , and  $E_a$  values confirm that the adsorption of methyl green onto MWCNTs decorated with  $\text{CoFe}_2\text{O}_4$  or  $\text{Co}_{0.5}\text{Ni}_{0.5}\text{Fe}_2\text{O}_4$  nanoparticles was a physisorption process. Lazaridis and Asouhidou [38] stated that in a diffusion-controlled process, the activation energy of adsorption was less than 25 to 30 kJ/mol. Based on the results of activation energy and the intraparticle diffusion model (Table 4 and Figure 9e,f), this study proposes that the adsorption involved intraparticle diffusion, that was not the only rate-controlling step, and the other kinetic models might control the adsorption rate.

## Conclusions

MWCNTs decorated with  $\text{CoFe}_2\text{O}_4$  and  $\text{Co}_{0.5}\text{Ni}_{0.5}\text{Fe}_2\text{O}_4$  nanoparticles have been successfully prepared by a hydrothermal precipitation method. The prepared composite exhibits a homogeneous dispersion of MWCNTs in the matrix and coating of  $\text{CoFe}_2\text{O}_4$  and  $\text{Co}_{0.5}\text{Ni}_{0.5}\text{Fe}_2\text{O}_4$  nanoparticles on MWCNTs. This study investigated the removal of methyl green from aqueous solution by the prepared composites. It was found that  $\text{Co}_{0.5}\text{Ni}_{0.5}\text{Fe}_2\text{O}_4/\text{MWCNTs}$  composite has a high adsorptive capacity than  $\text{CoFe}_2\text{O}_4/\text{MWCNTs}$  for methyl green adsorption. The equilibrium adsorption capacity of methyl green increased with the increase in temperature, methyl green concentration, and adsorbent materials. The adsorption kinetics could be quite successfully fitted by a pseudo-second-order kinetic equation. The Langmuir and Freundlich adsorption isotherm models were used to express the adsorption phenomenon of the methyl green. The equilibrium data were well described by the Langmuir model. Thermodynamic analyses indicated that the adsorption of methyl green onto MWCNTs decorated with  $\text{CoFe}_2\text{O}_4$  and

$\text{Co}_{0.5}\text{Ni}_{0.5}\text{Fe}_2\text{O}_4$  nanoparticles was endothermic, spontaneous, and physisorption process.

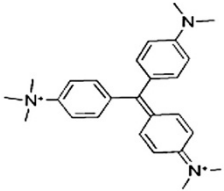
## Methods

### Material and methods

All the reagents were of analytical grade and used as received without further purification. Cobalt nitrate [ $\text{Co}(\text{NO}_3)_2 \cdot 6\text{H}_2\text{O}$ ], nickel nitrate [ $\text{Ni}(\text{NO}_3)_2 \cdot 6\text{H}_2\text{O}$ ], and ferric nitrate [ $\text{Fe}(\text{NO}_3)_3 \cdot 9\text{H}_2\text{O}$ ] were obtained from WINLAB, Baths, UK. Sodium hydroxide (NaOH) was obtained from Bio Chem Laboratories, Inc., Grand Rapids, MI, USA and methyl green (Table 5) was obtained from Gurr microscopy materials, BDH chemicals Ltd., Poole, England. MWCNTs were produced by chemical vapor deposition using acetylene cracking over Fe-Co/CaCO<sub>3</sub> catalyst/support. The method of synthesis had been described before [39]. The raw product contains the support, catalyst particles, and a few amorphous carbons as impurities. The as-grown MWCNTs were purified using a two-step purification procedure involving treatment with diluted HCl and then with mixture of concentrated nitric acid/sulfuric acid (3:1 by volume, respectively).

For the decoration of MWCNTs, a specific amount of oxidized MWCNTs was first ultrasonicated in 100 ml of distilled water for 30 min. Afterward, this suspension was mixed with a solution of analytical grade  $\text{Co}(\text{NO}_3)_2 \cdot 6\text{H}_2\text{O}$  and  $\text{Fe}(\text{NO}_3)_3 \cdot 9\text{H}_2\text{O}$  in which the Co/Fe molar ratio was maintained at 1:2, in case of decoration of MWCNTs with  $\text{CoFe}_2\text{O}_4$  nanoparticles. The mixture of  $\text{Ni}(\text{NO}_3)_2 \cdot 6\text{H}_2\text{O}$ ,  $\text{Co}(\text{NO}_3)_2 \cdot 6\text{H}_2\text{O}$  and  $\text{Fe}(\text{NO}_3)_3 \cdot 9\text{H}_2\text{O}$ , in which the Ni/Co/Fe molar ratio was maintained at 1:1:4, was used in case of decoration of MWCNTs with  $\text{Co}_{0.5}\text{Ni}_{0.5}\text{Fe}_2\text{O}_4$  nanoparticles. Then, a sodium hydroxide solution (6 molar) was added dropwise into the above mixture with vigorous stirring until the pH value reaches 10. The mixture was stirred for another 30 min for complete reaction then the solution was neutralized. The produced mixture was then placed in a Teflon-lined autoclave and maintained at 220°C for 10 h. The obtained precipitates were rinsed repeatedly with water and ethanol, and then, dried at 100°C for 12 h in a vacuum oven. The prepared powder was denoted as  $\text{CoFe}_2\text{O}_4/\text{MWCNTs}$  and  $\text{Co}_{0.5}\text{Ni}_{0.5}\text{Fe}_2\text{O}_4/\text{MWCNTs}$ .

**Table 5 Structure and characteristics of Methyl green dye**

Name	C.I. number	Formula	Molecular weight	$\lambda_{\text{max}}$	Chemical structure
Methyl green	42585	$\text{C}_{26}\text{H}_{33}\text{N}_3\text{Cl}_2$	458.5	630 to 634, 420 nm	

The synthesized and decorated MWCNTs were characterized by powder XRD analysis (D8 Advance, Bruker AXS, Inc, Madison, WI, USA), transmission electron microscopy (TEM, Jeol JEM-1230, Akishima-shi, Japan), and FTIR (JASCO 410, Mary's Court Easton, MD, USA). The BET surface area was determined from adsorption isotherms using a Quantachrome NOVA automated gas sorption system report.

#### Dye adsorption experiments

For studying the effect of dye concentration on the adsorption process equal volumes, 50 ml of various methyl green dye concentrations, were taken in number of 250-ml beakers. Definite weight of the adsorbent materials (CoFe<sub>2</sub>O<sub>4</sub>/MWCNTs or Co<sub>0.5</sub>Ni<sub>0.5</sub>Fe<sub>2</sub>O<sub>4</sub>/MWCNTs) was added in each beaker and shaken well. At different interval times, 5 ml of the sample solution was withdrawn and the change in characteristic absorption at the specific peaks was measured using an ultraviolet–visible (UV–vis) spectrophotometer (Jasco 530), from which the concentration of dye was inferred.

For evaluation, the effect of adsorbent materials concentration on the adsorption process equal volumes, 50 ml of definite methyl green dye concentrations, were taken in a number of 250-ml beakers. Different weights of the adsorbent materials were added in each beaker and shaken well. At different interval times, 5 ml of the sample solution was withdrawn and the change in characteristic absorption at the specific peaks was measured using an UV–vis spectrophotometer (Jasco 530), from which the concentration of dyes was inferred.

For identifying the adsorption isotherm and kinetics adsorption experiments were performed using 250-ml glass bottles, specific amount of the adsorbent materials were inserted into the bottles along with 50 ml of the methyl green dye solutions. The initial concentration of the dye (C<sub>0</sub>) was varied from 50 to 400 mg/L. The glass bottles were sealed and placed within a temperature control box to maintain water temperature. Temperatures that were studied include 298, 313, and 333 K. At the end of the equilibrium period, the suspensions were separated for later analysis of the dye concentration. The amount of dye adsorption at equilibrium  $q_e$  (mg/g) was calculated from the following equation:

$$q_e = V(C_0 - C_e) / W, \quad (11)$$

where C<sub>0</sub> and C<sub>e</sub> (mg/L) are the liquid-phase concentrations of methyl green dye at initial and equilibrium, respectively. V (L) is the volume of the solution, and W (g) is the mass of the used adsorbent. The concentration of the dye before and after adsorption was determined using a spectrophotometer (Jasco 530).

Kinetic experimental procedures were identical to the equilibrium tests. The effect of contact time on the amount of adsorbed methyl green dye was investigated at specific initial dye concentration and at varying temperatures (298, 313, and 333 K). The amounts of adsorbed dye on the adsorbent materials at any time,  $t$ , were calculated from the concentrations in solutions before and after adsorption. At any time, the amount of adsorbed dye (mg/g) onto the adsorbent materials was calculated from the mass balance equation as follows:

$$q_t = V(C_0 - C_t) / W, \quad (12)$$

where  $q_t$  is the amount of adsorbed dye on the adsorbent materials at any time (mg/g); C<sub>0</sub> and C<sub>t</sub> are the initial and liquid-phase concentrations of dye at any time (mg/L), respectively; V (L) is the volume of dye solution, and W (g) is the mass of the adsorbent materials.

#### Competing interests

The authors declare that they have no competing interests.

#### Authors' contributions

WR carried out the experimental part and wrote the manuscript for publication. AF participated in the idea and the design of the study. MB, MK, and AF as supervisors, participated in this work. All authors read and approved the final manuscript.

#### Acknowledgements

The authors gratefully acknowledge the financial support of this work by Beni-Suef University nanotechnology research team.

#### Author details

<sup>1</sup>Nanotechnology Department, Faculty of Postgraduate Studies for Advanced Sciences, Beni-Suef University, Beni-Suef 62111, Egypt. <sup>2</sup>Minerals Technology Department Central Metallurgical R & D Institute (CMRDI), Helwan 11421, Egypt.

Received: 26 April 2013 Accepted: 17 May 2013

Published: 15 July 2013

#### References

1. Tandon, S, Nandini, N: Adsorption efficiency of carbon prepared from agricultural waste materials in removing basic dye from aqueous solution. *Asian J. Chem.* **23**, 636–640 (2011)
2. Baskaran, P, Venkatraman, B, Arivoli, S: Kinetics of adsorption of ferrous ion onto acid activated carbon from *Zea mays* dust. *J. Chem.* **8**, 185–195 (2011)
3. Mohammadi, N, Khani, H, Gupta, VK, Amereh, E, Agarwal, S: Adsorption process of methyl orange dye onto mesoporous carbon material - kinetic and thermodynamic studies. *J. Colloid Interf. Sci.* **362**, 457–462 (2011)
4. Loghman, K, Salar, Z: Superior photocatalytic degradation of azo dyes in aqueous solutions using TiO<sub>2</sub>/SrTiO<sub>3</sub> nanocomposite. *J. Nanostruct. Chem.* **3**, 32 (2013)
5. Manoj Kumar Reddy, P, Rama Raju, B, Karupppiah, J, Linga Reddy, E, Subrahmanyam, C: Degradation and mineralization of methylene blue by dielectric barrier discharge non-thermal plasma reactor. *Chem. Eng. J.* **217**, 41–47 (2013)
6. Panic, VV, Madzarevic, ZP, Volkov-Husovic, T, Velickovic, SJ: Poly (methacrylic acid) Based Hydrogels as Sorbents for Removal of Cationic Dye Basic Yellow 28: Kinetics, Equilibrium Study and Image Analysis. *Chem. Eng. J.* **217**, 192–204 (2013)
7. Shi, Y, Kong, X, Zhang, C, Chen, Y, Hua, Y: Adsorption of soy isoflavones by activated carbon: kinetics, thermodynamics and influence of soy oligosaccharides. *Chem. Eng. J.* **215–216**, 113–121 (2013)
8. Machado, FM, Bergmann, CP, Fernandes, THM, Lima, EC, Royer, B, Calvete, T, Fagan, SB: Adsorption of Reactive Red M-2BE dye from water solutions by

- multi-walled carbon nanotubes and activated carbon. *J. Hazard. Mater.* **192**, 1122–1131 (2011)
9. Wang, JP, Yang, HC, Hsieh, CT: Adsorption of phenol and basic dye on carbon nanotubes/carbon fabric composites from aqueous solution. *Sep. Sci. Technol.* **46**, 340–348 (2011)
  10. Tang, WW, Zeng, GM, Gong, JL, Liu, Y, Wang, XY, Liu, YY, Liu, ZF, Chen, L, Zhang, XR, Tu, DZ: Simultaneous adsorption of atrazine and Cu (II) from wastewater by magnetic multi-walled carbon nanotube. *Chem. Eng. J.* **211–212**, 470–478 (2012)
  11. Plata, D, Gschwend, P, Reddy, C: Industrially synthesized single-walled carbon nanotubes: compositional data for users, environmental risk assessments, and source apportionment. *Nanotechnol.* **19**, 185706 (2008)
  12. Fraczek-Szczypta, A, Menaszek, E, Blazewicz, S: Some observations on carbon nanotubes susceptibility to cell phagocytosis. *J. Nanomat.* **2011**, 473516 (2011)
  13. Ngomsik, AF, Bee, A, Draye, M, Cote, G, Cabuil, V: Magnetic nano- and microparticles for metal removal and environmental applications: a review. *Comptes. Rendus. Chimie* **8**, 963–970 (2005)
  14. Yao, Y, Liu, S, Ma, LP, Sun, H, Wang, S: Synthesis, characterization, and adsorption properties of magnetic Fe<sub>3</sub>O<sub>4</sub>@ graphene nanocomposite. *Chem. Eng. J.* **184**, 326–332 (2012)
  15. Yao, Y, Miao, S, Ping Ma, L, Sun, H, Wang, S.: Fabrication of Fe<sub>3</sub>O<sub>4</sub>/SiO<sub>2</sub> core/shell nanoparticles attached to graphene oxide and its use as an adsorbent. *J. Colloid Interf. Sci.* **379**, 20–26 (2012)
  16. Konicki, W, Petech, I, Mijowska, E, Jasińska, I: Adsorption of anionic dye Direct Red 23 onto magnetic multi-walled carbon nanotubes-Fe<sub>3</sub>C nanocomposite: Kinetics, equilibrium and thermodynamics. *Chem. Eng. J.* **210**, 87–95 (2012)
  17. Qu, S, Huang, F, Yu, S, Chen, G, Kong, J: Magnetic removal of dyes from aqueous solution using multi-walled carbon nanotubes filled with Fe<sub>2</sub>O<sub>3</sub> particles. *J. Hazard Mater.* **160**, 643–647 (2008)
  18. Gong, JL, Wang, B, Zeng, GM, Yang, CP, Niu, CG, Niu, QY, Zhou, WJ, Liang, Y: Removal of cationic dyes from aqueous solution using magnetic multi-wall carbon nanotube nanocomposite as adsorbent. *J. Hazard Mater.* **164**, 1517–1522 (2009)
  19. Madrakian, T, Afkhami, A, Ahmadi, M, Bagheri, H: Removal of some cationic dyes from aqueous solutions using magnetic-modified multi-walled carbon nanotubes. *J. Hazard Mater.* **196**, 109–114 (2011)
  20. Bansal, RC: Activated Carbon Adsorption. Taylor and Francis Group. CRC Press, Boca Raton (2005)
  21. Bansal, RC, Goyal, M: Activated Carbon Adsorption. CRC Press, Boca Raton, Taylor and Francis Group (2005)
  22. Fugetsu, B, Satoh, S, Shiba, T, Mizutani, T, Lin, YB, Terui, N, Nodasaka, Y, Sasa, K, Kiyoko Shimizu, O, Akasaka, T: Caged multiwalled carbon nanotubes as the adsorbents for affinity-based elimination of ionic dyes. *Environ. Sci. Technol.* **38**, 6890–6896 (2004)
  23. Mall, ID, Srivastava, VC, Agarwal, NK: Removal of Orange-G and Methyl Violet dyes by adsorption onto bagasse fly ash—kinetic study and equilibrium isotherm analyses. *Dyes pigm.* **69**, 210–223 (2006)
  24. Langmuir, I: The adsorption of gases on plane surfaces of glass, mica and platinum. *J. Am. Chem. Soc.* **40**, 1361–1403 (1918)
  25. Freundlich, H: Over the adsorption in solution. *J. Phys. Chem.* **57**, 385–470 (1906)
  26. Hall, K, Eagleton, L, Acrivos, A, Vermeulen, T: Pore-and solid-diffusion kinetics in fixed-bed adsorption under constant-pattern conditions. *Ind. Eng. Chem. Fund.* **5**, 212–223 (1966)
  27. Wang, S, Boyjoo, Y, Choueib, A: A comparative study of dye removal using fly ash treated by different methods. *Chemosphere* **60**, 1401–1407 (2005)
  28. Haghseresh, F, Lu, G: Adsorption characteristics of phenolic compounds onto coal-reject-derived adsorbents. *Energ. Fuel.* **12**, 1100–1107 (1998)
  29. Demirbas, E, Dizge, N, Sulak, M, Kobya, M: Adsorption kinetics and equilibrium of copper from aqueous solutions using hazelnut shell activated carbon. *Chem. Eng. J.* **148**, 480–487 (2009)
  30. Weber, W, Morris, J: Kinetics of adsorption on carbon from solution. *J. Sanit. Eng. Div. J. Sanit. Eng. Div. Am. Soc. Civ. Eng.* **89**, 31–60 (1963)
  31. Ozcan, AS, Erdem, B, Ozcan, A: Adsorption of Acid Blue 193 from aqueous solutions onto Na-bentonite and DTMA-bentonite. *J. Colloid Interf. Sci.* **280**, 44–54 (2004)
  32. Zcan, A, Zcan, AS: Adsorption of Acid Red 57 from aqueous solutions onto surfactant-modified sepiolite. *J. Hazard Mater.* **125**, 252–259 (2005)
  33. Kannan, N, Sundaram, MM: Kinetics and mechanism of removal of methylene blue by adsorption on various carbons—a comparative study. *Dyes. pigm.* **51**, 25–40 (2001)
  34. Karagz, S, Tay, T, Ucar, S, Erdem, M: Activated carbons from waste biomass by sulfuric acid activation and their use on methylene blue adsorption. *Bioresour. Technol.* **99**, 6214–6222 (2008)
  35. Chen, C, Li, X, Zhao, D, Tan, X, Wang, X: Adsorption kinetic, thermodynamic and desorption studies of Th (IV) on oxidized multi-wall carbon nanotubes. *Colloid. Surface A.* **302**, 449–454 (2007)
  36. Doan, M, Alkan, M: Adsorption kinetics of methyl violet onto perlite. *Chemosphere* **50**, 517–528 (2003)
  37. Nollet, H, Roels, M, Lutgen, P, Van der Meer, P, Verstraete, W: Removal of PCBs from wastewater using fly ash. *Chemosphere* **53**, 655–665 (2003)
  38. Lazaridis, N, Asouhidou, D: Kinetics of sorptive removal of chromium (VI) from aqueous solutions by calcined Mg-Al-CO<sub>3</sub> hydrotalcite. *Water Res.* **37**, 2875–2882 (2003)
  39. Bahgat, M, Farghali, A, El Roubi, WMA, Khedr, M: Synthesis and modification of multi-walled carbon nano-tubes (MWCNTs) for water treatment applications. *J. Anal. Appl. Pyrol* **92**, 307–313 (2011)

doi:10.1186/2193-8865-3-50

Cite this article as: Farghali et al.: Decoration of multi-walled carbon nanotubes (MWCNTs) with different ferrite nanoparticles and its use as an adsorbent. *Journal Of Nanostructure in Chemistry* 2013 3:50.

Submit your manuscript to a SpringerOpen® journal and benefit from:

- Convenient online submission
- Rigorous peer review
- Immediate publication on acceptance
- Open access: articles freely available online
- High visibility within the field
- Retaining the copyright to your article

Submit your next manuscript at ► [springeropen.com](http://springeropen.com)